 CMC, vol.13, no.1, pp.1-15, 2009

Experimental and Numerical Study of Micro Deep Drawing of Copper Single Crystal

XL Geng[1], KS Zhang[2], YQ Guo[1] and L Qin[1]

Abstract: One of the problems in a micro-forming process is the grain size effect, which means the formed part consists of a single grain or several grains sometimes, so the material shows anisotropic or heterogeneous. Under these conditions, a conventional method, which based on the isotropic and homogeneous material hypothesis, is not suitable. In this paper, Experimental investigations into micro deep drawing of the copper single crystal were carried out and the pattern of the micro-cup and the drawing force were observed. Using crystal plasticity theory, a user material subroutine (VUMAT) was built and linked to ABAQUS, and the micro deep drawing was simulated according to the experimental configuration. The results show that earing occurs at mouth of the micro-cup. The profile, quantity, and location of ears depend on the crystalline orientation in the blank. The simulations are in good agreement with the experiments, which demonstrate that the crystal theory has the rationality and validity in micro-forming simulations.

Keywords: Crystal plasticity theory; Micro-forming; Plastic forming; Deep drawing; Earing

1 Introduction

The miniatures of products and micro machinery are developing rapidly, which bring widespread interest recently. Micro-forming process, as a micro-parts manufacturing method, has many characteristics such as high efficiency, mass-producing, short cycle, low cost and net forming, which ensure wide applications of microtechnique. Geiger, Kleiner et al (2001), Engel and Eckstein (2002), Vollertsen, Schulze and Hu (2006), made reviews of the problems associated with miniaturization, the way of the solution starting from basic research and some present progress. Messner, Engel et al (1994), Tiesler (2002), Vollertsen, Hu et al (2004) applied ex-

[1] Department of Engineering Mechanics, Northwestern Polytechnical University, Xi'an 710072, China
[2] College of Civil and Architectural Engineering, Guangxi University, Nanning 530004, China

periments and simulations to the micro-forming process and considered that the anisotropic material in the micro forming needs suitable treating.

As the ordinary metallic material is composed of a huge amount of grains, no individual grain could affect the whole material, so the conventional forming researches apply an isotropic and homogeneous hypothesis to the material, which omitted the special crystalline characteristics of an individual grain. A metallic grain usually has several symmetric crystalline planes, so it shows special anisotropic. When the size of a micro-part is at micron level, a part may only consist of several grains or a single grain. As a result, the material becomes anistropic or heterogeneous

The features above-mentioned exercise a considerable influence on the fabrication process and forming quality. Micro-forming needs to focus on the deformation of the individual grain and its physical mechanism of the deformation. In order to describe the plastic deformation in grains numerically, Taylor £¨1938£©created a crystal slip model, then Hill and Rice (1972), Asaro and Rice (1977), Peirce, Asaro and Needleman (1983) developed this model, built the algorithm and analyzed the parameters effect to the model. Hasebe (2006) presented recent achievements in field theoretical approach toward substantial linkage among key hieratical scales dominating polycrystalline plasticity of metals and alloys. Jayabal, Arockiarajan and Sivakumar (2008) proposed a three dimensional micromechanically motivated model to describe the nonlinear dissipative effects in the polycrystal ferroelectrics.

Many researchers presented numerical studies on forming processes by using crystal model. For example, Kim, Sim et al (2001), Ocenasek, Ripoll et al (2007) combined crystal constitutive relation and damage model to simulate rod tension. Becker, Smelser and Panchanadeeswaran (1993) Inala, Wu and Neale (2000), Miehe and Schotte (2004), Raabe, Wang and Roters (2005) applied crystal model to investigate the deep drawing process of copper and steel. The main goal of above simulations was to show the effects of crystal model and study the material texturing.

It's a suitable way to validate a numerical approach by a corresponding experiment. In this paper, the micro-forming process of copper single crystal was investigated by experiments and FEM simulations respectively. In the simulations, crystal plasticity theory, which based on the physical mechanism of the grain's plastic deformation, was used to describe the material behavior. Single crystal has simple crystalline feature and clear anisotropy. Thus, the researches on micro-forming of single crystal can lay a solid foundation for the subsequent work on micro-forming of multicrystal or polycrystal. This study aimed at gaining the relations between the profile of the micro-drawing cup and the crystalline orientation. The rationality and validity of the simulation method was inspected also.

2 Experiments

2.1 Material and specimen preparation

Copper single crystal (99.999% purity) was supplied in the form of directional solidification rod with diameter of 30mm. The orthogonal crystal orientations, [100] and [010] exist in the cross section; the [001] orientation is same as axial direction of the rod. The exact orientations in the rod had been marked by the material supplier (shown in Fig. 1). The blank was cut form the rod by wire EDM, then grinded and polished. Finally, the blank has the circular shape with diameter of 8mm and thickness of 0.3mm. When the blanks were put into the etching liquid ($FeCl_3$ 5g+HCl 15ml+H_2O 60ml), no grain boundary could be seen in the section (shown in Fig. 2), which demonstrated that the material is single crystal.

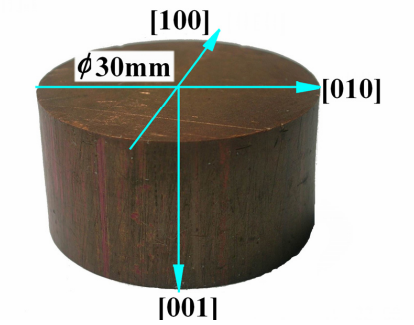

Figure 1: The copper single crystal ingot and it's crystal orientations.

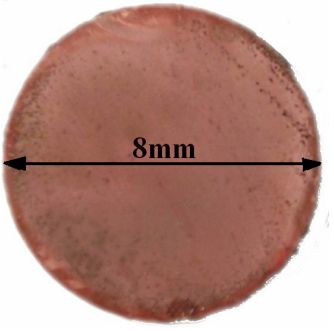

Figure 2: Metallograph of copper single crystal. No grain boundary exists.

2.2 Micro-forming mould

Deep drawing is the main process of plastic forming, which uses drawing mould to make the blank an open part. Fig. 3 shows the sketch of drawing a circular cup. The process could be described as following steps: Put the circular blank between die and blank holder; the punch move downwards; the diameter of the blank decreases with the blank being drawn into the mould; the flange of the blank form the perpendicular wall of the cup and the center part of the blank form the bottom of the cup. Based on the same principle, a mould was designed and built in this work, the important size of the mould is shown in Fig. 4, and the unit is mm.

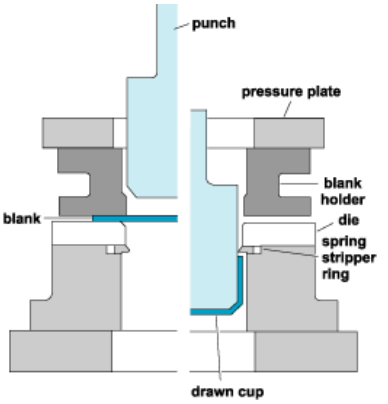

Figure 3: Sketch of the mould assembly.

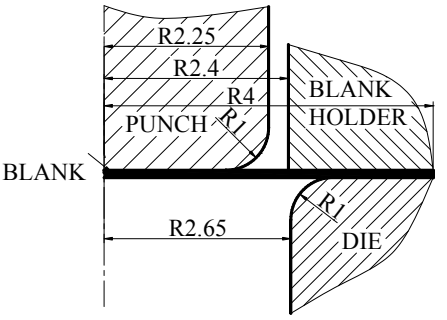

Figure 4: Geometry of drawing mould assembly.

2.3 Micro deep drawing experiments

The blank were marked with crystal orientations and ready for drawing. The orientation configuration is shown in Fig. 5.

Drawing direction is <100> orientation, the plane of the blank is {100}, was named <100>{100} set.

Drawing direction is <110> orientation, the plane of the blank is {110}, was named <110>{110} set.

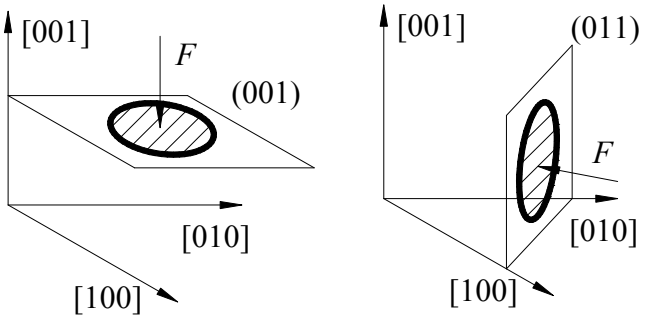

Figure 5: Sketch of deep drawing configuration of copper single crystal, ***F*** is punch force and the dark area is the blank.

The blanks were lubricated with MoS_2 grease and then they were put into the mould. The mould was laid on INSTRON 5567, a universal material testing ma-

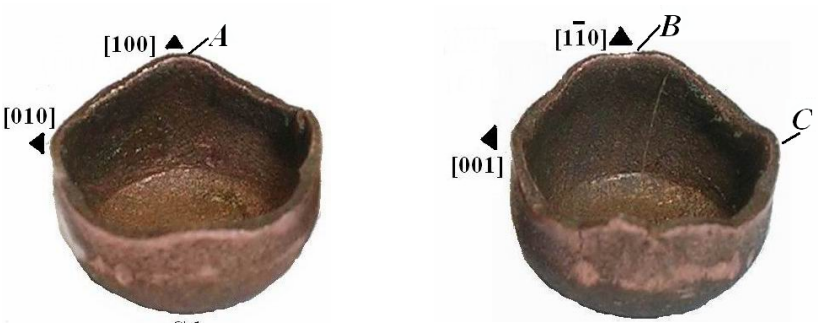

(a) The drawn micro-cup of <100>{100} set (b) The drawn micro-cup of <110>{110} set

Figure 6: The appearance of micro-cup of copper single crystal with different orientation

chine. The movement speed of the punch was set to 5mm/min. Fig. 6 shows the drawn cups with two different crystalline orientations respectively. <100>{100} set has four same ears at <100> crystalline orientation, whereas <110>{110} set has four ears, the two ears at <110> direction are big and they have local sags (see point *B*, Fig. 6(b)), the others at <100> direction are small (see point *C*).

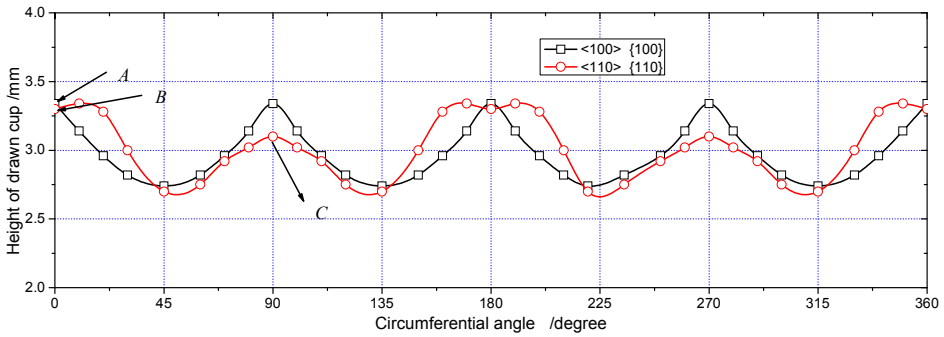

Figure 7: The earing profile curve of copper single crystal with different orientation

Fig. 7 illustrates the measured earing profile curves. The horizontal axis is circumferential angle of the cup. The original point of the coordinate axis is point *A* or *B* (see Fig. 6), and the angle increases counterclockwise. The vertical axis is the distance from bottom of the cup to ear margin. From this figure, the effect of the crystalline orientation on the ear pattern could be observed. The two curves are very different but the heights of two ears are similar, about 0.7mm.

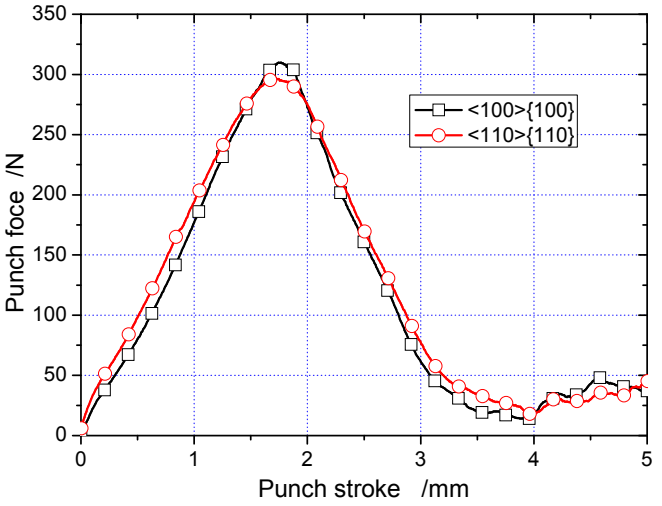

Figure 8: The punch force vs. punch stroke of copper single crystal with different orientations

Fig. 8 shows that no remarkable distinction was found in the punch forces of two blanks which are of the same size but different crystal orientations. The punch forces reach to maximum when punch stroke equals 1.7mm, which is corresponding to the most materials of the blank bearing plastic deformation; therefore, a large resisting force has to be overcome by the punch. After that, while the blank is dragged into the mould by the punch continuously, the plastic deformation trends to end, so the punch force drops. When the punch stroke reaches 3.5mm, the blank has been dragged into the mold completely. The little remaining punch force is the reaction to friction between the micro-cup and inside wall of the mould.

3 Crystal plasticity theory

The basic crystal plasticity model frame described by Asaro and Rice (1972), Peirce, Asaro and Needleman (1983). We applied this model to simulate the deep drawing process of copper single crystal. The total deformation of a crystal is the result of two distinct physical mechanisms: crystallographic slip due to dislocation motion on the active slip systems, and elastic lattice distortion. The numerical algorithm, which suggested by Zhang, Wu and Feng (2005), was used to integrate the incremental theory.

The deformation of crystals can be categorized into elastic and plastic parts. In the

crystallographic axis coordinate, they can be expressed in the rate form as follows

$$\dot{\boldsymbol{\varepsilon}} = \dot{\boldsymbol{\varepsilon}}^e + \dot{\boldsymbol{\varepsilon}}^p \tag{1}$$

$$\dot{\boldsymbol{\sigma}} = \mathbf{C} : \dot{\boldsymbol{\varepsilon}}^e \tag{2}$$

Where $\dot{\boldsymbol{\varepsilon}}$ is total strain rate, $\dot{\boldsymbol{\varepsilon}}^e$ is the elastic $\dot{\boldsymbol{\varepsilon}}^p$ the plastic strain rate, $\mathbf{C}$ the four order elastic tensor and the symbol ":" means inner product.

The evolution of the plastic strain rate has the relationship with all slip systems' movements, and the expression can be written as

$$\dot{\boldsymbol{\varepsilon}}^p = \sum_{\alpha=1}^{n} \mathbf{P}^{(\alpha)} \cdot \dot{\gamma}^{(\alpha)} \tag{3}$$

where α is the order number of the slip system, $P^{(\alpha)}$is the Schimid tensor of the slip system, n the quantity of the slip systems, to FCC copper, $n = 12$. Hutchinson (1976) suggested a power law for the resolved shearing strain rate, in which the slip rate on α-slip system can be written as

$$\dot{\gamma}^{(\alpha)} = \dot{\gamma}_0 (\frac{\tau^{(\alpha)}}{g^{(\alpha)}}) \left| \frac{\tau^{(\alpha)}}{g^{(\alpha)}} \right|^k \tag{4}$$

where $\dot{\gamma}_0$ is the reference rate of shearing strain (taken as a material constant), k the rate sensitivity parameter, and $\tau^{(\alpha)}$ the resolved shear stress, and $g^{(\alpha)}$ is the scalar function describing the state of strain hardening. The evolution equation for $g^{(\alpha)}$ is

$$\dot{g}^{(\alpha)} = \sum_{\beta=1}^{n} h_\beta^\alpha \left| \dot{\gamma}^{(\beta)} \right| \tag{5}$$

where h_β^α is the slip-plane hardening rates with the diagonal terms representing "self-hardening" on a slip system and the off-diagonal terms representing "latent hardening":

$$h_\beta^\alpha = qh(\gamma) + (1-q)h(\gamma)\delta_\beta^\alpha \tag{6}$$

where q is the latent ratio, δ_β^α the Kronecker symbol and the $h(\gamma)$has the following form

$$h(\gamma) = h_0 \sec h^2 (\frac{h_0 \gamma}{g_s - g_0}) \tag{7}$$

where h_0 is the initial hardening rate, g_0 the initial critical resolved shear stress (CRSS), g_s is the saturation value of the shear stress and γ is obtained with the following expression:

$$\gamma = \int \sum_{\beta}^{n} \left| d\gamma^{(\beta)} \right| \tag{8}$$

Based on the theory above, we implemented the algorithm to a VUMAT (User material subroutine). The subroutine was applied to describe the material behavior of the blank and then connected the subroutine with ABAQUS (2001). The parameters of the crystal model was obtained and calibrated by tensile test of same material.

Table 1: Parameters of the crystal plasticity model

$\dot{\gamma}_0(\mathrm{s}^{-1})$	k	q	h_0 (MPa)	g_0 (MPa)	g_s (MPa)	C_{11} (MPa)	C_{12} (MPa)	C_{44} (MPa)
0.001	50	1.4	62	22.2	100.4	168400	121400	75400

4 Numerical simulations

4.1 Finite element model of deep drawing

According to the scheme of the experiment, the finite model of the blank was built with solid elements. The finite element model of the punch assembly is shown in Fig. 9. The punch, die and blank holder were built as rigid parts.

According to the experimental conditions, the contact between blank and mould was treated as follows: the inner surface of the die contacted with lower surface of the blank; the punch contacted with the upper surface of the blank; the blank holder contacted with the upper surface of the blank; we defined the contacting surfaces as contact pair. Following the Coulomb friction concept, we set the tangential friction condition by giving suitable frictional coefficient μ. As no lubrication existed between punch and blank, assume μ=0.3, whereas there were good lubrication used between die-blank pair and blank holder-blank, thus μ=0.1. The blank holder pressed against the blank with 100N constant force, which could increase the blank rigidity and prevent wrinkling. As no accurate experimental data about friction and blank holder force were obtained, the corresponding data applied in the FEM was estimated empirically by referring to Rabbe, Zhao and Roters (2001), Raabe and Roters (2004), Zhao, Mao et al (2004). The deep drawing process was accomplished through punch moving downwards 5mm, then the blank was drawn as a micro-cup.

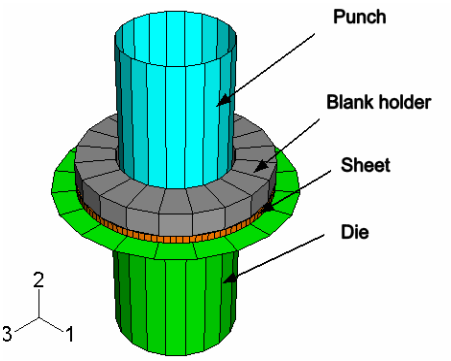

Figure 9: The mould assembly scheme in FEM

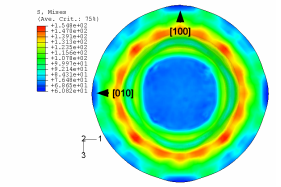

(a) Mises stress，s=1mm

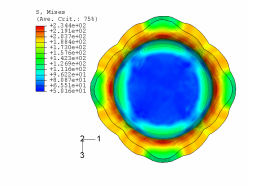

(b) Mises stress，s=2mm

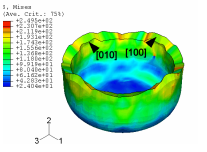

(c) Mises stress，s=3mm

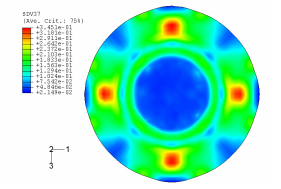

(d) ε_{eq}^{p}，s=1mm

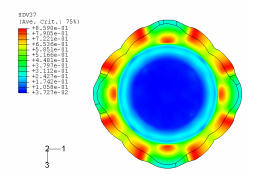

(e) ε_{eq}^{p}，s=2mm

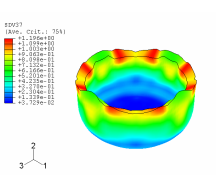

(f) ε_{eq}^{p}，s=3mm

Figure 10: Mises stress and Equivalent plastic strain (ε_{eq}^{p}) distribution at different punch stroke (s), the <100>{100}set

4.2 Simulation of deep drawing of <100>{100} set

Define {100} crystal plane as the plane to be punched and <100> crystal orientation as the direction of punch force. The equivalent plastic strain and stress distribution of the cup at different punching depth (s) are shown in Fig. 10. When s=1mm, the maximum stress is produced at contacting region with chamfering of the die. In this place, the blank material bears circumferential compressive stress, radial tensile stress and severe friction with the die. The maximum plastic deformation occurs along <100> crystal orientation on the flange. The distribution characteris-

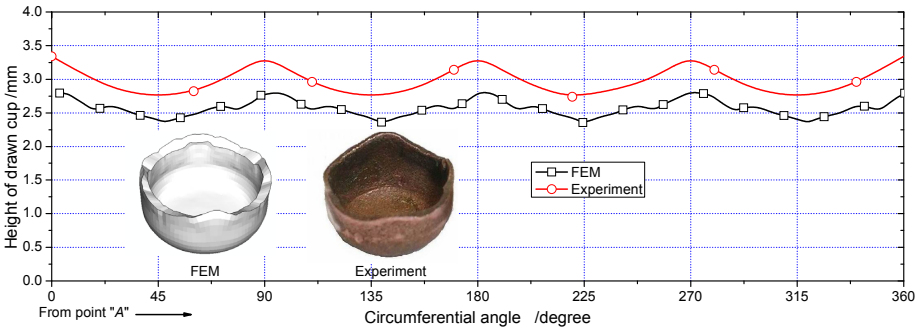

Figure 11: Earing and cup appearance. Comparison of simulation with experimental data, the <100>{100}set

tics of stress and strain reflect the crystal orientation varying in the blank regularly. Moreover, it is the demonstration of anisotropy of the single crystal material. When s=2mm, the margin of the flange become square. Finally, the blank forms a cup with four same ears, which exist in <100> orientations. These phenomena could not be seen in conventional forming of isotropic material, in which the strain distribution in an isotropic material would be uniform at same radius, thus no earing would be produced.

Fig. 11 shows the comparisons between the experiment and simulation. The experimental earing is a little higher than simulated one, which results from limited description ability of the model. The two curves show same pattern and ear locations. In the same figure, we can see that the micro-cup obtained in simulation corresponds to the experimental one very well.

The simulated punch force is similar with experimental one (see Fig. 12). The conformability in cup appearance indicates the applicability of crystal plasticity theory, and the conformability in punch force demonstrates the finite element model is reasonable. Fig. 13 shows that local thickness of the cup increasing dramatically (near troughs of the cup, as marked), which prevents the blank from being dragged into the mould and leads to punch force fluctuating at the descending stage in simulation results.

4.3 Simulation of deep drawing of <110>{110} set

The equivalent plastic strain and stress distribution and the cup pattern at different depth (s) is shown in fig.14. When s=2mm, the edge profile of the blank is nearly a diamond-shaped. The long axis is along $[1\bar{1}0]$ orientation, whereas the short axis is along [100] orientation. In the end, the micro-cup earing occur at two orienta-

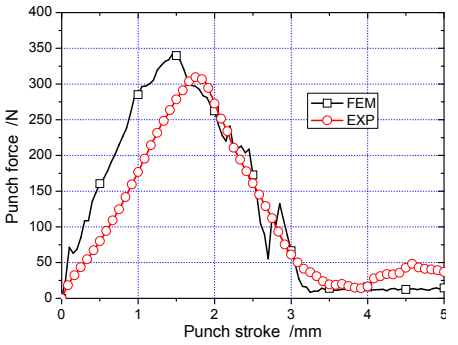

Figure 12: Comparison of punch force between simulation and experiment data, the <100>{100}set

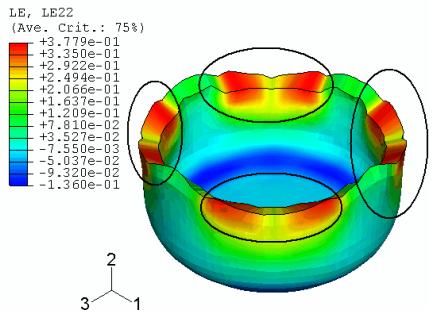

Figure 13: Thickness strain distribution of the <100>{100}set

tions, the bigger ears locate in $[1\bar{1}0]$ orientation and the smaller one locate in [100] orientation.

Fig. 15 shows comparison of ear profile obtained by the simulation and experiment. The two curves had good similarity. The appearances of the simulated and experimental cups show good agreement.

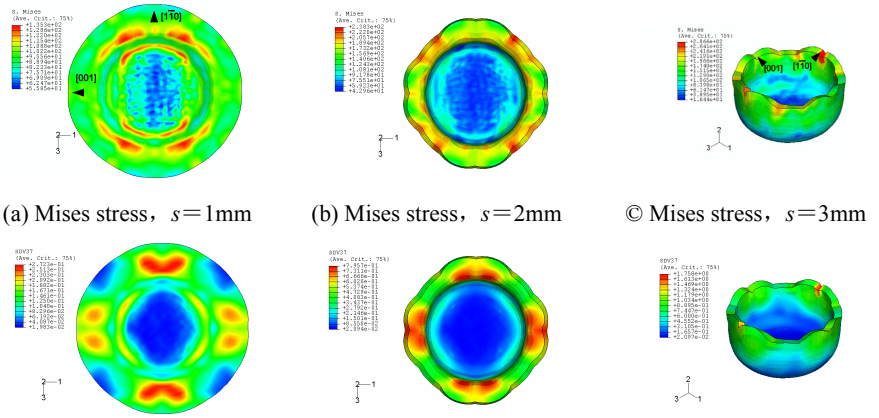

(a) Mises stress，s=1mm (b) Mises stress，s=2mm © Mises stress，s=3mm

(d) ε_{eq}^{p}，s=1mm (e). ε_{eq}^{p}，s=2mm (f) ε_{eq}^{p}，s=3mm

Figure 14: Mises stress and Equivalent plastic strain (ε_{eq}^{p}) distribution at different punch stroke (s), the <110>{110}set

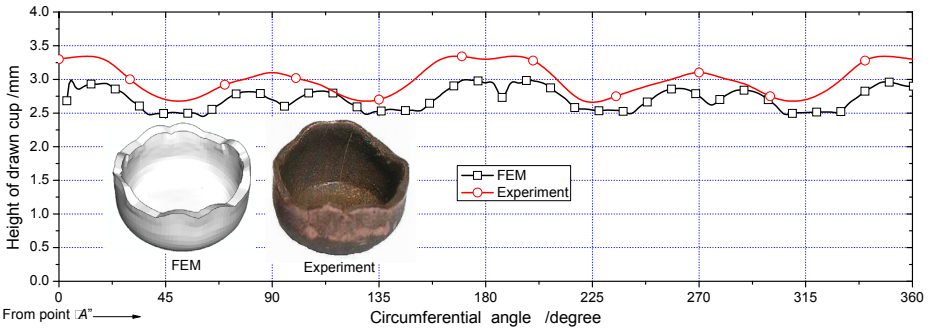

Figure 15: Earing and cup appearance. Comparison of simulation with experimental data, the <110>{110}set

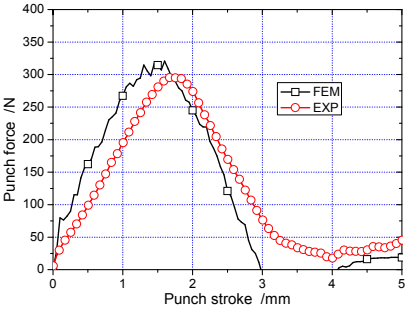

Figure 16: Comparison of punch force between simulation and experimental data, the <110>{110}set

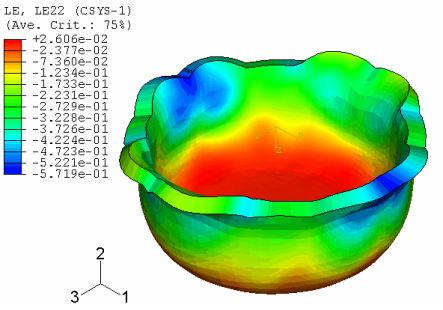

Figure 17: Thickness strain distribution of the <110>{110}set

Fig. 16 compares the punch force obtained by the experiment and simulation. It is noticed that no fluctuating occurs in descending branch as the local thickness only increases a little (see Fig. 17), which does not affect the subsequent movement of the blank.

5 Concluding Remarks

In the experiments, copper single crystal blanks with different crystalline orientation were drawn into a mould to produce micro-cups. The punch force and the earing profile were observed. According to the experimental configuration, the crystal plasticity FE method was applied to simulate cup deep drawing. Through the analysis and comparison between simulated and experimental results, some conclusions

can be drawn:

1. The experiments show that the profile of the earing depends on the crystal orientation of the blank. The number of the ears is determined by the crystal symmetries in the blank. If {100} crystal plane is the blank plane, four same ears are produced in <100> orientation; If {110} crystal plane is the blank plane, two big ears are produced in <110> orientation and two small ears produced in <100> orientation. The punch force curves of two crystal orientations have similarity.

2. According to the real configuration, the FE method combining with crystal plasticity theory were used to simulate deep drawing of single crystalline blank. The simulated results are in good agreement with experiment in micro cup appearance, earing profile, earing location and punch force. Consequently, crystal plasticity has been demonstrated to have a good ability in describing plastic forming of crystal material, whose advantages cannot be substituted by classical isotropic plastic models. The outlook for this work is to study plastic forming of materials consisting of several grains, which has more importance and universality in micro-forming.

Acknowledgement: The authors are grateful to support of the National Natural Science Foundation of China (Grant Nos. 10472092 and 10662001)

References

Geiger, M.; Kleiner, M.; Eckstein, R.; Tiesler, N.; Engel, U. (2001): Microforming, *51st General Assembly of CIRP*, Nancy, vol. 50, pp. 445-462.

Engel, U.; Eckstein, R. (2002): Microforming-from basic research to its realisation, *Journal of Materials Processing Technology.* vol. 125–126, pp. 35-44.

Vollertsen, F.; Schulze, N. H.; Hu, Z. (2006): State of the art in micro forming, *International Journal of Machine Tools & Manufacture*, vol. 46, pp. 1172-1179.

Messner, A.; Engel, U.; Kals, l. R.; vollertsen, F. (1994): Size effect in the FE-simulation of micro-forming processes, *Journal of Materials Processing Technology*, vol.45, pp. 371-376.

Tiesler, N. (2002): *Grundlegende Untersunchungen zum Fliebpressen metallischer* Kleinstteile, M. Geiger, K. Feldmann(eds.), Reihe Fertigungstechnik Erlangen, Band 132, Meisenbach, Bamberg,

Vollertsen, F.; Hu, Z.; Niehoff, H. S.; Theiler, C. (2004): State of the art in micro forming and investigations into micro deep drawing, *Journal of Materials Processing Technology* vol. 151, pp. 70-79.

Taylor, G. L. (1938): Plastic strain in metals, *J. Inst. Metals.* vol. 62, pp. 307-324.

Hill, R.; Rice, J. R. (1972): Constitutive analysis of elastic-plastic crystal at arbitrary strain. *J Mech Phys Solids*, vol. 20, pp. 401-413.

Asaro, R. J.; Rice, J. R. (1977): Strain localization in ductile single crystals. *J Mech Phys Solids*, vol. 25, pp. 309-338.

Peirce, D.; Asaro, R. J.; Needleman, A. (1983): Material rate dependence and localized deformation in crystalline solids. *Acta Metall.*, vol. 31, pp. 1951-1976.

Hasebe, T. (2006): Multiscale crystal plasticity modeling based on field theory, *CMES: Computer Modeling in Engineering and Sciences*, vol. 11, pp. 145-155.

Jayabal, K.; Arockiarajan, A.; Sivakumar, S.M. (2008): A micromechanical model for poly crystal ferroelectrics with grain boundary effects, *CMES: Computer Modeling in Engineering and Sciences,* vol. 27, pp. 111-123.

Kim, Y.I.; Sim, K.S.; Yoh, E.G.; Lee,Y.S.; Park, H.J.; Na, K.H. (2001): Analysis of the milli-forming of single-crystal and poly-crystal bar, *Journal of Materials Processing Technology*, vol. 113, pp. 70-74.

Ocenasek, J.; Ripoll, M. R.; Weygand, S.M.; Riedel, H. (2007): Multi-grain finite element model for studying the wire drawing process, *Computational Materials Science*, vol. 39, pp. 23-28.

Becker, R.; Smelser, R. E.; Panchanadeeswaran S. (1993): Simulations of earing in aluminum single crystals and Polycrystals, *Modelling Simul. Mater. Sei. Eng.*, vol. 1, pp. 203-224.

Inala, K.; Wu, P.D.; Neale, K.W. (2000): Simulation of earing in textured aluminum sheets, *International Journal of Plasticity*, vol. 16, pp. 635-648.

Miehe, C.; Schotte, J. (2004): Anisotropic finite elastoplastic analysis of shells: simulation of earing in deep-drawing of single- and polycrystalline sheets by Taylor-type micro-to-macro transitions, *Comput. Methods Appl. Mech. Engrg.*, vol. 193, pp. 25-57.

Raabe, D.; Wang,Y.; Roters, F. (2005): Crystal plasticity simulation study on the influence of texture on earing in steel, *Computational Materials Science*, vol. 34, pp. 221-234.

Zhang, K.S.; Wu, M.S.; Feng, R. (2005): Simulation of microplasticity-induced deformation in uniaxially strained ceramics by 3-D Voronoi polycrystal modeling, *International Journal of Plasticity*, vol. 21, pp. 801–834.

Hutchinson, J.W. (1976): Bounds and self-consistent estimates for creep of polycrystalline materials , *Proc. Roy. Soc. Lond.* vol. 348A, pp. 101-127.

ABAQUS Reference Manuals (2001): V6.2., Hibbit, Karlsson & Sorenson.

Raabe, D., Zhao, Z., Roters, F. (2001): A finite element method on the basis of texture components for fast predictions of anisotropic forming operations, *Steel Res.*, vol. 72, pp. 421–426.

Raabe, D.; Roters, F. (2004): Using texture components in crystal plasticity finite element simulations, *International Journal of Plasticity*, vol. 20, pp. 339-361.

Zhao, Z.; Mao, W., Roters, F., Raabe, D. (2004): A texture optimization study for minimum earing in aluminium by use of a texture component crystal plasticity finite element method, *Acta Mater.*, vol. 52, pp. 1003-1012.